Effect of Surfactants on the Minimum Miscible Pressure of CO_2 with Crude oil from the Chang-8 Oilfield using Molecular Dynamics Simulation

Zhenzhen Dong, Tong Hou, Zhanrong Yang, Lu Zou, Weirong Li*, Xi'an Shiyou University, Xi'an, China; **Keze Lin**, China University of Petroleum (Beijing), Beijing, China; **Hongliang Yi**, Petrochina Liaohe Oilfield Company, Panjin, China; **Zhilong Liu**, EnerTech-Drilling & Production Co., CNOOC Energy Technology & Services Ltd

Abstract

CO_2 flooding represents a promising approach for enhancing the recovery of tight reservoirs, facilitating the efficient development of unconventional oil and gas resources while concurrently contributing to CO_2 reduction. This method is of significant importance for the sustainable advancement of energy in China. Both theoretical and empirical evidence indicate that the oil recovery efficiency associated with CO_2 miscible-phase processes markedly exceeds that of non-miscible-phase processes. However, current CO_2 injection technologies often struggle to achieve miscible-phase conditions in various contexts, thus limiting their effectiveness in enhancing recovery from tight reservoirs.

The composite system formed by CO_2 and surfactants presents a novel avenue for optimizing CO_2 flooding technology aimed at improving recovery of tight reservoirs. In this study, a molecular system model was established to characterize the interaction between CO_2 and crude oil specific to the Chang 8 tight reservoir. Molecular dynamics simulations were employed to estimate the miscibility pressure. The surfactant $C_{12}PO_6$ was introduced to investigate its impact on physical parameters, including intermolecular forces, interfacial tension, and miscible pressure, within the CO_2-crude oil-surfactant system.

The findings demonstrate that the incorporation of surfactants enhances molecular interactions between CO_2 and crude oil, resulting in a reduction of minimum miscibility pressure by 9.36% at a temperature of 344 K. Furthermore, the extent of this reduction is temperature-dependent, with a 10% increase in surfactant efficacy observed as the temperature rises from 323 K to 363 K. This research elucidates the interactions among multiple fluid molecules at the molecular level, revealing the microscopic mechanisms by which the CO_2-surfactant composite system reduces miscibility pressure in tight reservoirs. These insights are poised to advance the development of CO_2 enhanced recovery technologies within China's tight oil and gas sector.

Introduction

The greenhouse effect and the increasing global energy demand have emerged as critical issues. In this context, CO_2 gas flooding has gained considerable attention for its dual benefits (Gozalpour et al. 2005; Peng et al. 2022). It not only enhances the recovery of oil and gas resources, thereby extending the lifespan of limited energy supplies, but also aids in CO_2 sequestration, contributing to the reduction of atmospheric CO_2 emissions and mitigating the greenhouse effect on Earth's climate (Ju et al. 2012).

Improved Oil and Gas Recovery

DOI: 10.14800/IOGR.1314

Received August 17, 2024; revised September 1, 2024; accepted September 19, 2024.

*Corresponding author: weirong.li@xsyu.edu.cn

The mechanisms by which CO_2 increases oil and gas recovery primarily involve two processes: immiscible flooding and miscible flooding. In immiscible flooding, the reservoir pressure is below the minimum miscibility pressure (MMP), preventing CO_2 from fully mixing with the oil and resulting in a phase interface. In contrast, miscible flooding occurs when the reservoir pressure exceeds the MMP, allowing complete mixing of oil and gas, thus enhancing the efficiency of CO_2 flooding for improved oil recovery. Studies indicate that recovery rates from miscible flooding are significantly higher than those from immiscible flooding (Mian et al. 2018; Fath and Pouranfard 2014). However, many oil reservoirs in China exhibit relatively low formation pressures, and the crude oil often has high viscosity and a substantial content of heavy components, posing challenges to achieving the MMP necessary for CO_2 miscible flooding. Consequently, realizing miscible CO_2 flooding presents a significant challenge.

To facilitate CO_2 miscible flooding, one strategy is to increase formation pressure through gas or water injection until it reaches or surpasses the MMP. However, this approach may lead to reservoir fracturing. Therefore, researchers have started investigating the use of specific chemical additives to modify the phase behavior of CO_2 and crude oil, thereby reducing the MMP and promoting the miscible flooding process. Notable chemical additives include alcohols, fatty acids, and surfactants (Almobarak et al. 2021).

Alcohols, as nonpolar solvents, can enhance the viscosity and density of CO_2 while simultaneously reducing the viscosity and density of crude oil (Li et al. 2003), lowering interfacial tension between CO_2 and crude oil, which aids in their mixing and promotes miscibility (Djabbarah et al. 1988). Yang et al. (2019) employed the interfacial tension disappearance method to study the impact of adding 5 wt% primary alcohols (1-butanol, 1-pentanol, and 1-hexanol) on CO_2 solubility in the CO_2-crude oil system. Their results indicated that the solubility of CO_2 increased with pressure, and the addition of alcohols improved CO_2 solubility in heavy crude oil components. Additionally, the introduction of a mixed alcohol led to a 9.21% reduction in minimum miscibility pressure compared to the absence of alcohol (Rudyk et al. 2013).

Fatty acids, characterized by a hydrophobic hydrocarbon chain and a polar carboxyl tail (Voon and Awang 2014), also enhance CO_2 solubility in crude oil due to the presence of polar functional groups. Qayyimah et al. (2016) utilized the slim tube method to assess the effects of fatty acid methyl esters (FAME) on MMP in CO_2-oil systems. Their experiments revealed a 4% reduction in MMP with the addition of 5 vol% FAME at pressures ranging from 18 to 31 MPa. However, the emulsifying capacity of fatty acids remains suboptimal, even at high concentrations.

Surfactants are amphiphilic compounds with a hydrophilic head and a hydrophobic tail. They reduce MMP in CO_2 flooding through several mechanisms: (1) enhancing CO_2's interaction with heavy components, thereby increasing CO_2 solubility in crude oil (Qi et al. 2016); (2) disrupting the equilibrium between liquid and gas phases to enhance CO_2 extraction from crude oil; (3) adsorbing onto crude oil surfaces, thereby decreasing intermolecular forces and viscosity (Yang et al. 2015); and (4) interacting with both crude oil and CO_2 to reduce interfacial tension and promote miscibility (Miao et al. 2013). Surfactants can be categorized based on their hydrophilic heads into anionic, cationic, nonionic, and amphoteric types. Traditional anionic and cationic surfactants exhibit poor solubility in supercritical CO_2, hindering micelle formation.

Guo et al. (2017) investigated the influence of a synthesized oil-soluble surfactant (CAE) on MMP using the slim tube method at pressures of 18-30 MPa and 85°C, finding a 6.1 MPa (22%) reduction in MMP with a pre-slug of 0.2 wt%. Lou et al. (2018) examined the effects of nonionic surfactants in a CO_2 flooding system, reporting a reduction in MMP from 19.1 MPa to 13.8 MPa (27.7%) with 0.6 wt% of a propoxylated surfactant. Wang et al. (2016) demonstrated that fatty alcohol polyoxypropylene ethers effectively reduce miscibility pressure, achieving a significant reduction when the hydrophobic chain length was 12 and the hydrophilic functional group had a degree of polymerization of 6 ($C_{12}PO_6$). Under specific conditions (0.6 wt% $C_{12}PO_6$, 0.7 wt% ethanol, and 333.15 K), MMP was reduced from 17.79 MPa to 13.22 MPa, indicating a decrease of over 26%.

In summary, among various chemical additives, nonionic surfactants, particularly $C_{12}PO_6$, have shown notable efficacy in lowering MMP. However, the exact mechanisms by which $C_{12}PO_6$ reduces interfacial

tension remain inadequately understood. This study employs molecular dynamics simulations to explore the mechanisms through which $C_{12}PO_6$ reduces interfacial tension, comparing MMP and interfacial properties before and after its addition, with a focus on molecular structure and fundamental force fields. The paper is structured as follows: the introduction reviews methods and the current state of research on reducing miscibility pressure between CO_2 and crude oil; the second section outlines fundamental theories and research methods; the third section delves into surfactants' mechanisms affecting CO_2 and crude oil miscibility; and the final section presents discussion and conclusions.

Methodology

This study utilized molecular dynamics simulations conducted with the LAMMPS (Large-scale Atomic/Molecular Massively Parallel Simulator) software, originally developed by Sandia National Laboratories in 1984. LAMMPS is an open-source package specifically designed for large-scale atomic and molecular parallel simulations. The motion trajectories and instantaneous structural representations of all models were visualized and analyzed using the OVITO software.

Molecular Model. To accurately replicate the miscibility process between crude oil and CO_2 , the molecular dynamics model of crude oil was developed based on the actual composition of reservoir components. The composition consists of 24.90% C_1, 30.93% C_2, 9.54% C_{8+}, 19.59% C_{11+}, and 15.05% C_{23+}. This study focuses on linear aliphatic structures, excluding the consideration of their complex isomeric forms. All alkanes are constructed using a united-atom model, where hydrogen atoms are combined with their adjacent carbon atoms to form unified atoms. This simplification in the force field model balances model efficiency with the accurate representation of molecular structure and properties (Dong et al. 2022; Qu et al. 2022). The molecular models of each component are depicted in **Figure 1**.

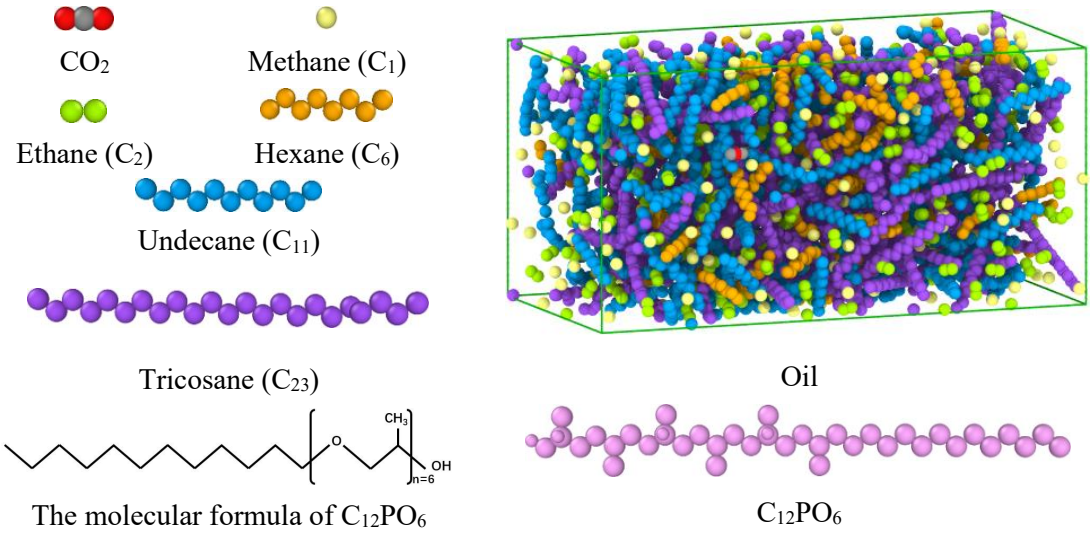

Figure 1—Each individual molecular model/crude oil model.

The selection of an appropriate molecular force field is a critical step in molecular simulations, as it directly influences the accuracy of the results. In constructing this model, CO_2 molecules were represented using the ZHU force field (Zhu et al. 2009), a flexible and computationally efficient model particularly suitable for systems involving supercritical CO_2. The CH_4 molecules in the crude oil were modeled with the TraPPE-UA (Transport Properties of Pure and Polymeric Compounds) force field (Nath et al. 1998; Martin and Siepmann 1998). Surfactant molecules were described using the OPLS-UA (Optimized Potential for Liquid Simulations-

United Atoms) force field (Jorgensen et al. 1996), while the remaining crude oil components (C_2, C_8, C_{11}, C_{23}) were modeled using the NERD force field (Wang et al. 2018; Nath et al. 1998).

$$U(r_{ij}) = 4\varepsilon_{ij}\left[\left(\frac{\sigma_{ij}}{r_{ij}}\right)^{12} - \left(\frac{\sigma_{ij}}{r_{ij}}\right)^{6}\right] + \frac{q_i q_j}{4\pi r_{ij}} \quad (1)$$

where, ε_{ij} represents the depth of the potential well; σ_{ij} represents the distance at which the interaction energy between two particles is minimal; r_{ij} is the distance between particles i and j; while q_i and q_j denote the partial charges for particles i and j, respectively.

By employing mixing rules, Lennard-Jones (Lennard-Jones 1931) parameters for various atomic interactions can be calculated. In this simulation, the commonly employed Lorentz-Berthelot combination rule is utilized (Stanishneva-Konovalova and Sokolova 2015),

$$\sigma_{ij} = \frac{\sigma_{ii} + \sigma_{jj}}{2} \quad (2)$$

$$\varepsilon_{ij} = \sqrt{\varepsilon_{ii}\varepsilon_{jj}} \quad (3)$$

The force field parameters used for the simulations in this paper are outlined in **Table 1**(Qian et al. 2024).

Table 1—Molecular force field parameters.

Molecular	Atom	σ_{ij} (nm)	ε_{ij} (KJ•mol^{-1})	change(e)	Model
CO_2	C	0.2757	0.2339	0.6512	ZHU
	O	0.3	0.6690	-0.3256	
n-decane	CH_3	0.3910	0.8647	0	NERD
	CH_2	0.3930	0.3808	0	
CH_4	CH_4	0.3730	1.2300	0	TraPPE-UA
Fatty alcohol Ether $C_{12}PO_6$	C(in CH-OR bond)	0.35	0.2761	0.17	OPLS-UA
	C(in C-OH bond)	0.35	0.2761	0.205	
	CH_2(in CH_2-OR bond)	0.38	0.4937	0.25	
	CH_2(in C-C bond)	0.3905	0.4937	0	
	CH_3(in C-C bond)	0.3905	0.7322	0	
	O(in C-OH bond)	0.312	0.7114	-0.683	
	O(in C-O-C bond)	0.3	0.7113	-0.5	
	H(in O-H bond)	0	0	0.418	

Simulation Details and Analysis Methods. All simulation units established in this study were configured using periodic boundary conditions in the x, y, and z directions. To replicate reservoir conditions, the simulation temperature was controlled within the range of 50 to 90 degrees Celsius. The simulation box dimensions automatically adjusted to their optimal sizes under varying temperature and pressure conditions through molecular simulations. As initial molecular models often deviate significantly from equilibrium, a series of preparatory steps was performed before the simulations. First, the models underwent energy minimization using the conjugate gradient method to achieve minimal energy and optimized configurations. Subsequently, initial velocities were randomly assigned to the atoms according to the Maxwell-Boltzmann distribution. The equations of motion were solved using the Verlet integration method (Li et al. 2023).

Thermodynamic ensembles are essential in molecular dynamics, enabling the study of macroscopic system properties by conducting multiple simulations under varying conditions to gather data. The most common ensembles include the microcanonical ensemble (NVE), canonical ensemble (NVT), isothermal-isobaric ensemble (NPT), and isobaric-isenthalpic ensemble (NPH). In this study, both the NVT and NPT ensembles were employed. The NPT ensemble maintains a constant number of particles (N), pressure (P), and temperature (T) during the simulation. Similarly, in the NVT ensemble, the number of particles (N) and temperature (T) remain constant, while the volume (V) is held fixed.

The simulation process began with NPT simulations to equilibrate the system's properties, ensuring a stable state of energy, temperature, and pressure. This was followed by control over the system using the NVT ensemble. Trajectory data was recorded at 1 ps intervals, and data points were generated every 1 fs for further analysis. In NPT simulations, temperature control was achieved via the Nosé-Hoover thermostat with a relaxation time of 200 fs (Hoover et al. 1982; Nosé 1984). For systems involving CO_2, long-range electrostatic interactions were calculated using the Particle-Particle Particle-Mesh (PPPM) method (Hockney et al. 1989), with an accuracy of 10^{-5}. A cutoff radius of 20 Å was employed, and the time step was fixed at 1 fs.

The results from molecular dynamics simulations were analyzed by observing trajectories, generating radial distribution functions, density distribution curves, and measuring interfacial tension.

Trajectories Analysis. Trajectory analysis entails capturing the positions and velocities of each atom in the system at every time step during molecular simulations. This data is subsequently processed using software tools such as OVITO, which generates visualizations of instantaneous trajectories, providing an intuitive representation of particle motion throughout the simulation. This method is crucial for gaining insights into the dynamic behavior, energy, and thermodynamic properties of the system's individual particles (Stukowski et al. 2009).

Radial Distribution Function (***RDF***). The RDF is a key metric for describing the spatial distribution relationships between different atoms or molecules in a system. It is defined as the ratio of the probability of finding a particular atom or molecule within a given spatial volume at a distance 'r' to the probability of finding the same atom or molecule in a randomly distributed system within the same volume. RDF is an invaluable tool for exploring intermolecular forces and interactions between atoms or molecules (Mo et al. 2014).

$$g(r) = \frac{dN}{\rho 4\pi r^2 dr} \quad \text{.....(4)}$$

where N represents the number of particles in the system; ρ denotes the particle density within the system, measured in units of g/cm^3; and r represents the distance between two particles, measured in Ångströms (Å).

Density Distribution Curve. The density distribution curve provides a visual representation of particle aggregation across different positions within the system, accurately illustrating particle distribution at various time intervals. It is particularly useful in reducing inaccuracies caused by sampling and measurement errors, ensuring a more reliable depiction of particle behavior within the simulated environment.

Interfacial Tension (***IFT***). Interfacial tension is a critical parameter used to describe the properties of an interface between two phases (Rao 1997). In molecular simulations, the pressure tensor is calculated in different directions within the system, and the IFT is subsequently derived by integrating the appropriate equation (e.g.,

Eq. 5). This method enables a precise estimation of the system's interfacial tension, offering insight into phase behavior and surface properties.

$$\gamma = \frac{1}{2}\int_0^{L_z}\left(P_N(z) - P_T(z)\right)dz = \frac{1}{2}\left[P_{zz} - \frac{P_{xx}+P_{yy}}{2}\right]L_z \quad \text{.....(5)}$$

where γ represents the interfacial tension; $P_N(z)$ and $P_T(z)$ denote the normal and tangential pressures, respectively. $P_{\alpha\alpha}(\alpha = x, y, z)$ is the quantity along the diagonal of the pressure tensor, and L_z is the length in the Z direction of the simulated system.

Results

Molecular Dynamics Simulation of the CO_2 and Crude Oil System. As shown in **Figure 2(a)**, the initial setup of the simulation consists of 1000 CO_2 molecules positioned on both sides, with 800 crude oil molecules centered between them. The CO_2-crude oil system is examined under two pressure conditions: 13.5 MPa (non-miscible) and 19.5 MPa (miscible). The system's structural evolution is analyzed at different time intervals during the simulation.

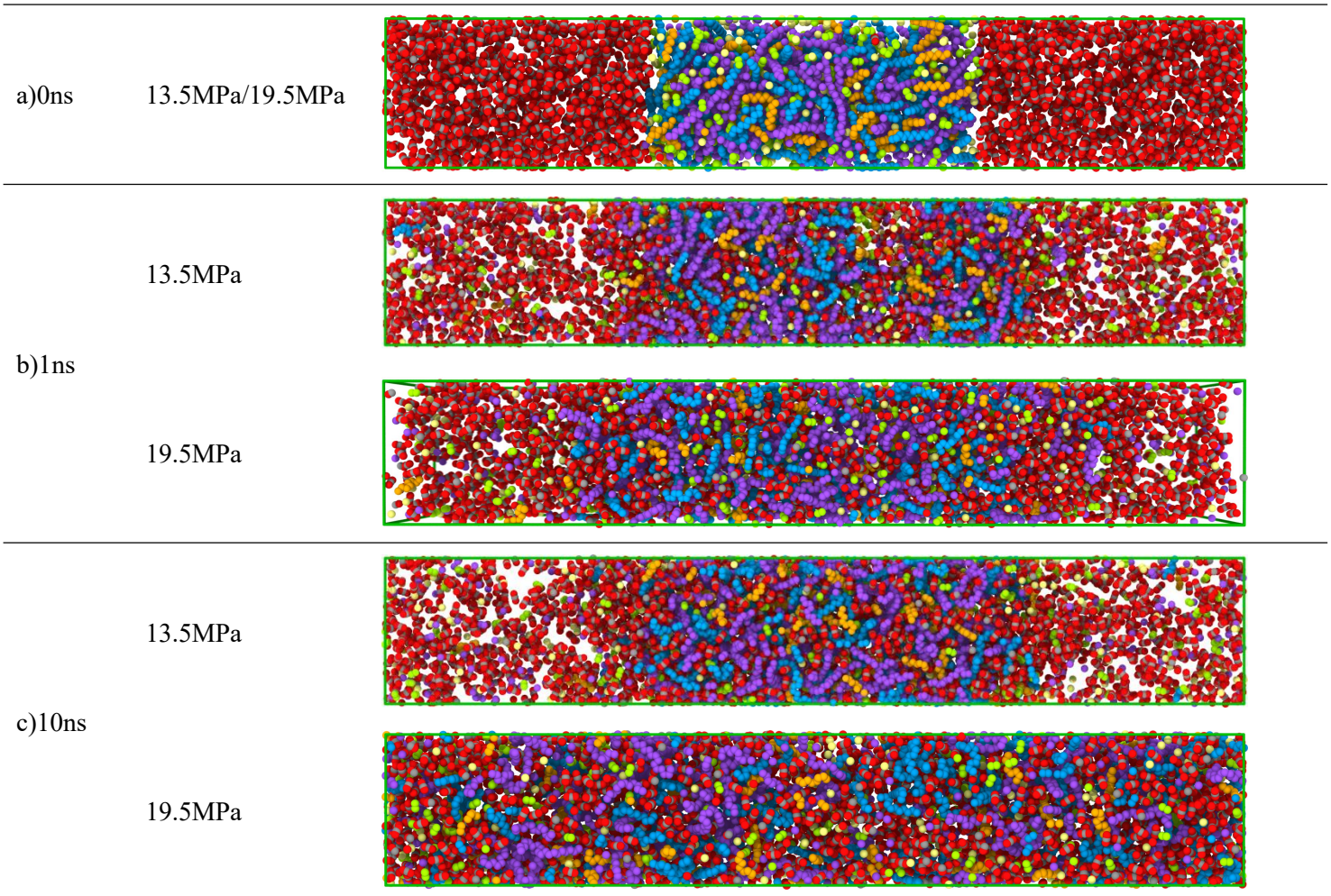

Figure 2—Instantaneous structures of the CO_2-crude oil system at various time steps (13.5MPa/19.5MPa).

At 13.5 MPa, the initial configuration reveals CO_2 molecules occupying the outer regions, with crude oil components located centrally, forming a distinct oil-gas interface. After 1 ns, the crude oil begins to diffuse outward, while CO_2 starts dissolving into the oil. However, due to the pressure being significantly lower than the miscibility threshold, the diffusion of both CO_2 and crude oil remains limited over time, resulting in minimal CO_2 dissolution within the system.

In contrast, at 19.5 MPa, the system exhibits a different progression. As time advances, CO_2 molecules from the outer regions infiltrate the central zone containing crude oil. This interaction leads to CO_2 enveloping the crude oil molecules, and the oil diffuses towards the system's periphery, broadening the phase interface. With prolonged simulation time, the solubility of CO_2 in crude oil increases, resulting in the formation of CO_2 clusters around crude oil molecules. This ultimately causes the phase interface to vanish, indicating that the system has reached miscibility.

A comparison of the structural snapshots at both pressure conditions highlights a significant difference. At 1 ns, the oil-gas interface at 19.5 MPa is broader than that at 13.5 MPa, primarily due to the higher pressure enhancing CO_2 solubility within the crude oil system. The stronger interactions between CO_2 and crude oil at 19.5 MPa result in faster diffusion. By 10 ns, the interface in the lower-pressure system remains largely unchanged, whereas in the higher-pressure system, the oil and gas have become fully miscible.

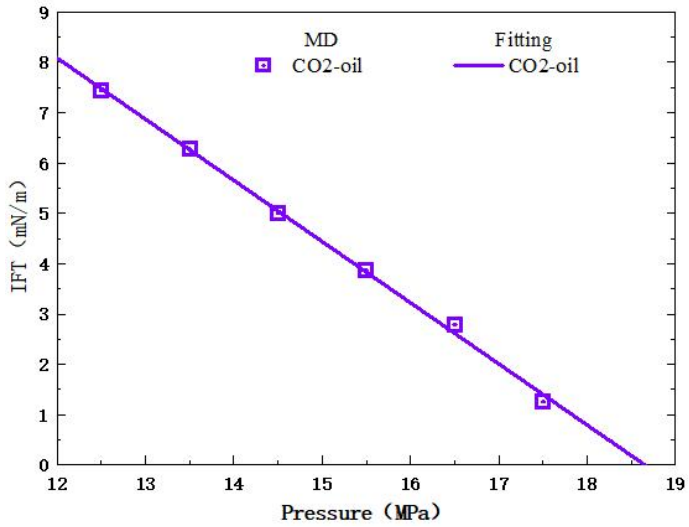

Figure 3—The variation of interfacial tension in CO_2-crude oil systems with pressure.

Minimum Miscibility Pressure Determination. The minimum miscibility pressure (MMP) between CO_2 and crude oil at a temperature of 344 K was established using the interfacial tension (IFT) disappearance method. By calculating the IFT at varying pressure levels, a relationship between interfacial tension and pressure was plotted, as shown in **Figure 3**. The graph clearly indicates a linear relationship between IFT and pressure, where the interfacial tension decreases as the pressure increases.

Through linear regression analysis, the following equation was obtained to describe this relationship,

$$IFT=-1.22P+22.67, \quad (6)$$

where IFT is the interfacial tension in mN/m; P is the pressure in MPa.

According to this linear model, when the interfacial tension reaches zero, the minimum miscibility pressure (MMP) is determined. Setting IFT to 0 in the equation yields,

$$0=-1.22P+22.67 \quad (7)$$

Solving for P, the MMP is found to be 18.65 MPa. This value signifies the pressure at which CO_2 and crude oil become miscible, a critical parameter for processes such as enhanced oil recovery (EOR).

Molecular Dynamics Simulation of Surfactant-Mediated Reduction in CO_2 Flooding Miscibility Pressure. This study employs $C_{12}PO_6$ as the selected surfactant for molecular dynamics simulations, aiming to investigate the variations in minimum miscibility pressure of the CO_2 and crude oil system before and after the surfactant's incorporation. The objective is to elucidate the mechanisms that contribute to the reduction of minimum miscibility pressure. In this section, the simulation framework consists of crude oil situated at the center, flanked by CO_2 molecules on either side, with a monolayer of surfactant molecules bridging the oil and gas phases. The oil components comprise a total of 800 molecules, consistent with the specifications outlined in the preceding section. Each monolayer is composed of eight $C_{12}PO_6$ molecules, while the system contains a total of 2000 CO_2 molecules, with 1000 positioned on each side.

Initially, within the NPT ensemble, the system's density is gradually equilibrated to a stable state over a total simulation duration of 25 ns. Subsequently, the simulation transitions to the NVT ensemble for a 10 ns equilibrium sampling period, during which data is collected once the system attains equilibrium in both energy and temperature.

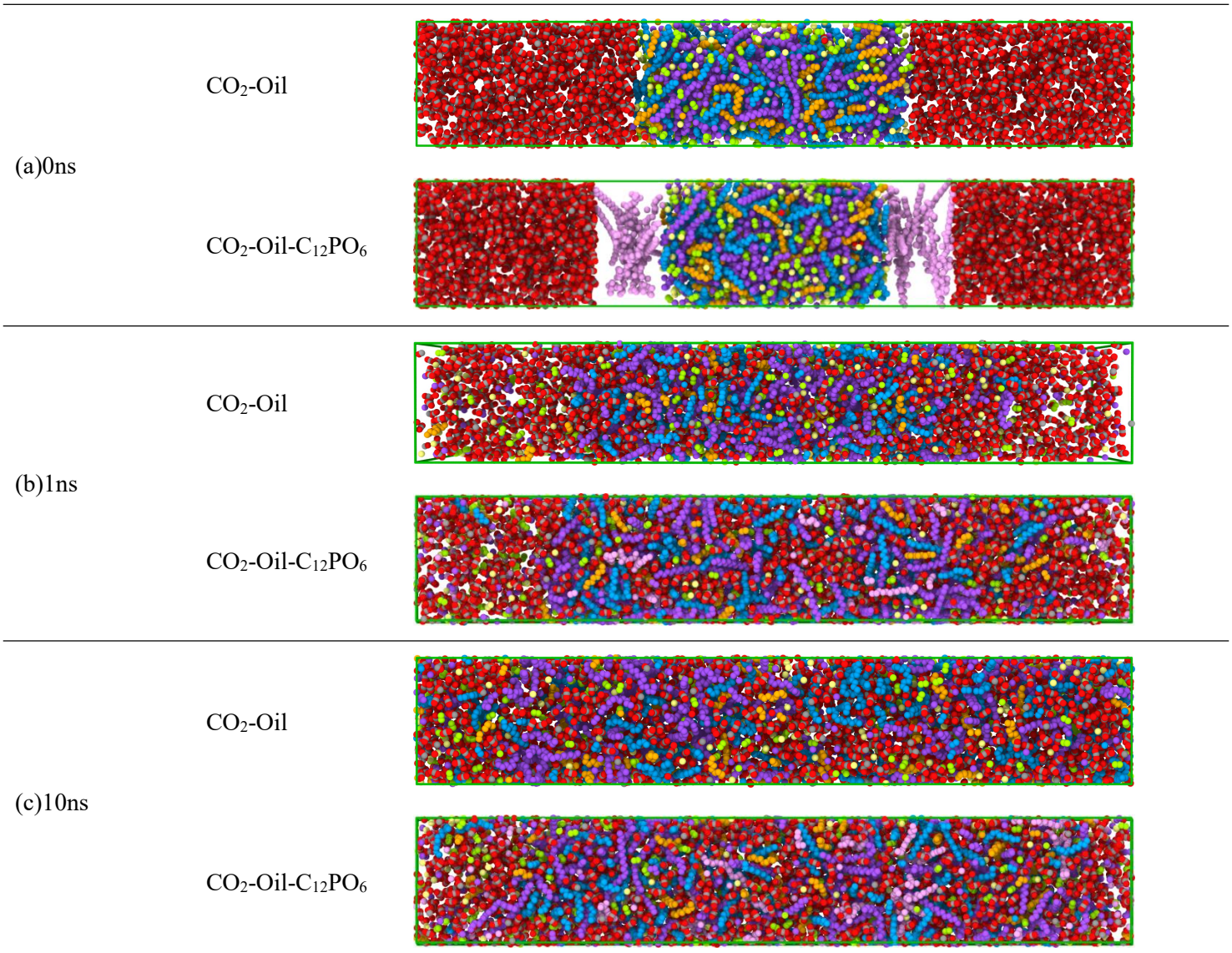

Figure 4—Instantaneous structure of the CO_2/crude oil/$C_{12}PO_6$ system at various time steps (@19.5 MPa).

At a pressure of 19.5 MPa, comparisons are made of the instantaneous structural snapshots of the simulation system at various time points before and after the addition of the surfactant. **Figure 4(a)** illustrates the initial configurations of both systems. Over time, CO_2 molecules are observed to dissolve into the crude oil at the center of the system, while crude oil molecules migrate towards the periphery (**Figure 4(b)**). It is evident that following the addition of the surfactant, the interface between the oil and gas phases becomes significantly wider compared to the scenario without the surfactant. This observation can be attributed to the surfactant's enhancement of CO_2 dissolution rates, facilitating a more rapid and complete mutual dissolution of the two phases. By the 10 ns mark (**Figure 4(c)**), both systems are observed to have reached a state of miscibility.

Using the interface disappearance method, a series of simulations were conducted on the CO_2-crude oil system following the incorporation of the surfactant, with a constant temperature maintained while varying the pressure. As illustrated in **Figure 5**, the introduction of $C_{12}PO_6$ results in a reduction of interfacial tension within the CO_2-crude oil system. This finding indicates that the $C_{12}PO_6$ surfactant plays a significant role in enhancing the miscibility of CO_2 with crude oil.

The linear relationship between pressure and interfacial tension can be expressed by the fitted equation,

$$IFT = -1.42P+24.01 \quad (8)$$

Based on this relationship, it can be inferred that the system's minimum miscibility pressure is 16.9 MPa when the interfacial tension approaches zero. This signifies a reduction of 9.36% in the minimum miscibility pressure.

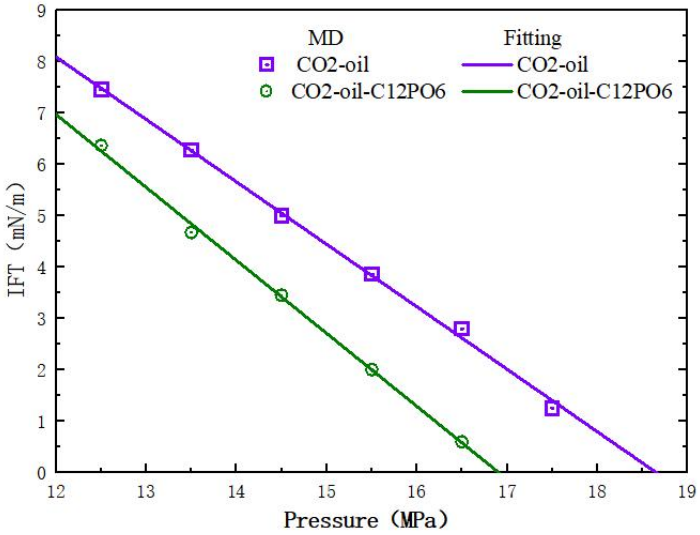

Figure 5—Changes in interfacial tension in the CO_2-crude oil system before and after surfactant addition.

Figure 6 illustrates the density distribution of various substances at the specified temperature and pressure. The density distribution curves for C_1, C_2, C_8, and CO_2 exhibit relative uniformity across the system. In contrast, the curves for C_{11}, C_{23}, and $C_{12}PO_6$ display a uniform central region with a declining trend toward both ends, resulting in a distribution that is slightly narrower than the overall width of the system. This behavior can be attributed to the achievement of miscibility throughout the system; lighter components such as C_1, C_2, C_8, and CO_2 are evenly distributed due to sufficient dissolution, thereby occupying the entire available space.

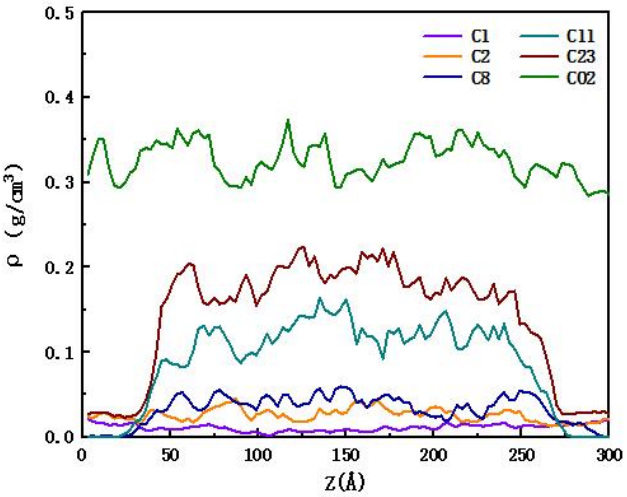

Figure 6—Density distribution curves before and after the addition of C12PO6.

Conversely, heavier components like C_{11} and C_{23} possess higher viscosity and density, which hinders the dissolution of CO_2 within them. As a result, during the phase-mixing process, these heavier components struggle to permeate the entire system uniformly. **Figure 7** presents the density distribution of the heavier components under two conditions: with and without the surfactant. At the miscibility pressure, neither scenario achieves a completely uniform distribution of C_{11} and C_{23} within the system. However, a comparative analysis reveals that the presence of the surfactant facilitates a more favorable distribution and diffusion of C_{11} relative to C_{23}. This observation is attributed to the lighter mass of C_{11}, which enhances its diffusion under the influence of the surfactant.

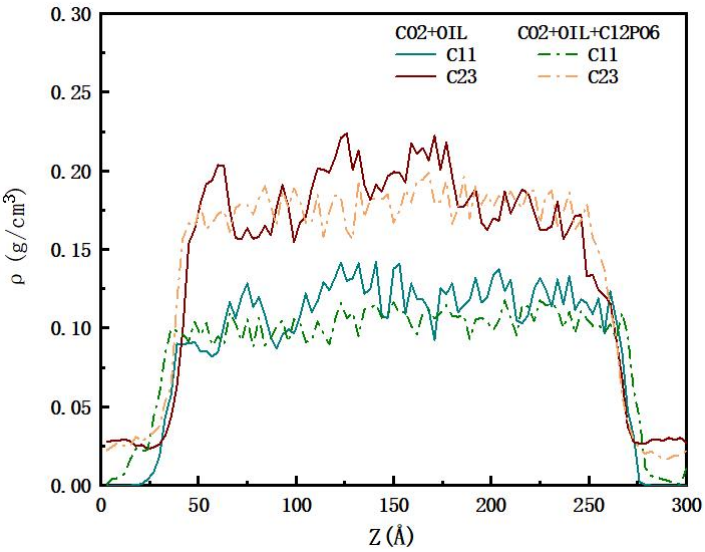

Figure 7—The density distribution of heavy components before and after the addition of surfactant.

Molecular dynamics simulations provide a detailed characterization of the phase interface properties between CO_2 and the oil system, which are often difficult or impossible to observe using traditional experimental methods. Due to the diversity of oil components and the significant variations in their concentrations, individual analyses may introduce considerable uncertainty. Consequently, when assessing the density distribution of the oil and gas phases, all six oil phase components are grouped together and collectively referred to as 'OIL' to ensure a consistent analysis of density distribution.

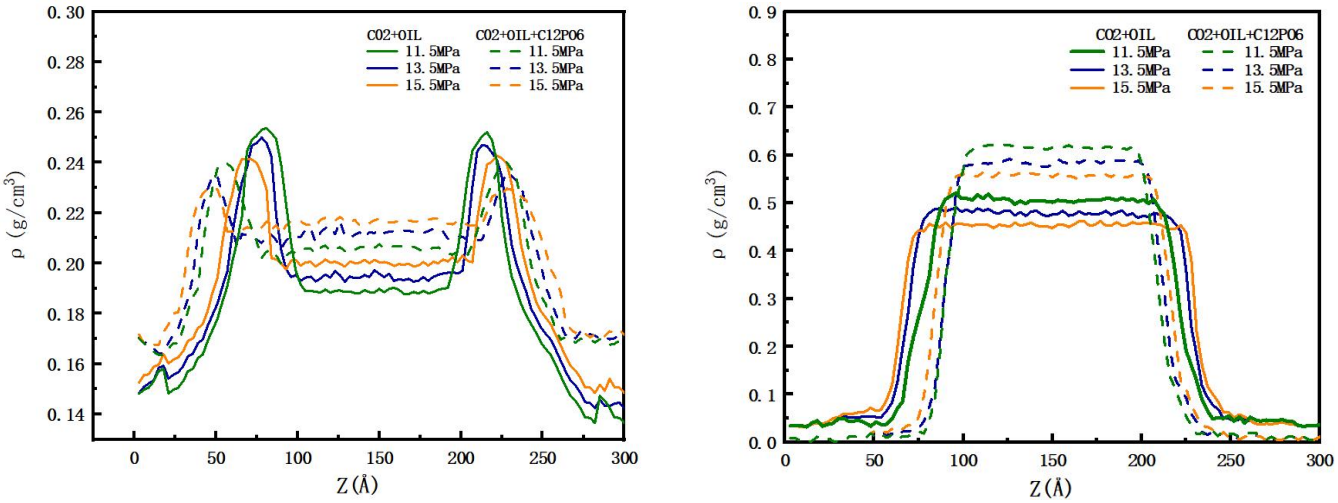

(a) CO_2 density distribution (b) Crude oil density distribution

Figure 8—CO_2 and crude oil density distribution before and after the addition of surfactant (344K).

Figure 8 illustrates the density distribution curves of CO_2 and crude oil both before and after the addition of surfactant. Under the same pressure conditions within the CO_2-crude oil system, the introduction of surfactant results in a decrease in the density of crude oil while simultaneously increasing the density of CO_2 within the oil phase. This expansion in oil volume indicates that CO_2 can dissolve more effectively in the crude oil, ultimately contributing to a reduction in the minimum miscibility pressure between the oil and gas. As pressure increases, the density of CO_2 in the oil gradually rises, suggesting that elevated pressure enhances the dissolution of CO_2 in the crude oil. Concurrently, the density of crude oil in the central region of the system decreases due to the increased pressure causing crude oil to disperse towards the system's edges, which leads to an expansion of the volume occupied by the crude oil.

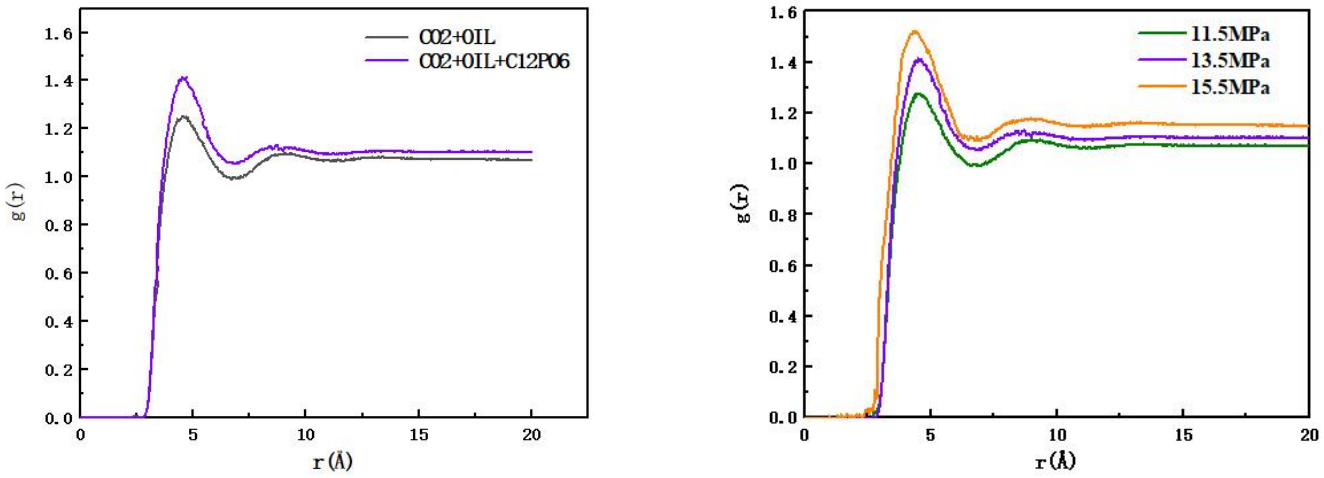

(a) Before and after the addition of $C_{12}PO_6$ (13.5MPa, 344K) (b) The system after the addition of $C_{12}PO_6$ (344K)

Figure 9—Radial distribution functions of CO_2-oil before and after adding $C_{12}PO_6$/radial distribution functions of co_2-oil in the system after the addition of $C_{12}PO_6$ as a function of pressure.

Figure 9(a) presents the radial distribution functions of CO_2 and crude oil molecules, both with and without the surfactant, under conditions of 344 K and 13.5 MPa. This graphical representation provides insights into the interactions between these components. A comparative analysis of the two curves reveals that the introduction of surfactants under identical conditions results in a steeper distribution curve with higher peaks. This observation indicates a significant enhancement of the interaction forces between CO_2 and crude oil, facilitating increased CO_2 solubility in the crude oil. Thus, the addition of surfactants alters the intermolecular forces between oil and gas molecules, subsequently affecting the solubility of CO_2 in crude oil.

Figure 9(b) depicts the radial distribution functions between CO_2 and crude oil molecules within the CO_2-crude oil-$C_{12}PO_6$ system at varying pressures of 11.5, 13.5, and 15.5 MPa. As pressure increases, the peaks of these radial distribution functions become more pronounced. This trend signifies that, at higher pressure levels, the intermolecular forces between CO_2 and crude oil molecules strengthen, leading to enhanced solubility of CO_2 in the crude oil.

Effect of Temperature on the Efficiency of Surfactant. Reservoir temperature is a critical determinant of the minimum miscibility pressure in CO_2 flooding processes. To encompass the temperature range observed in the examined reservoirs, this chapter performs molecular dynamics simulations on oil and gas systems at three distinct temperatures: 323 K, 344 K, and 363 K.

The accompanying graph illustrates the variations in interfacial tension within the CO_2 and crude oil system as a function of temperature. It is evident that, at lower pressures, interfacial tension decreases with rising temperature, whereas at higher pressures, interfacial tension increases with temperature. By utilizing the linear relationship between pressure and interfacial tension, specific pressure-interfacial tension equations were formulated for different temperatures. Ultimately, we calculated the minimum miscibility pressure, corresponding to the point at which interfacial tension approaches zero, as shown in Figure 10. These results indicate that minimum miscibility pressure increases with rising temperature. Without the addition of surfactant, the minimum miscibility pressure escalates from 12.808 MPa at 323 K to 18.65 MPa at 363 K. In contrast, with surfactant inclusion, it rises from 12.13 MPa to 18.06 MPa.

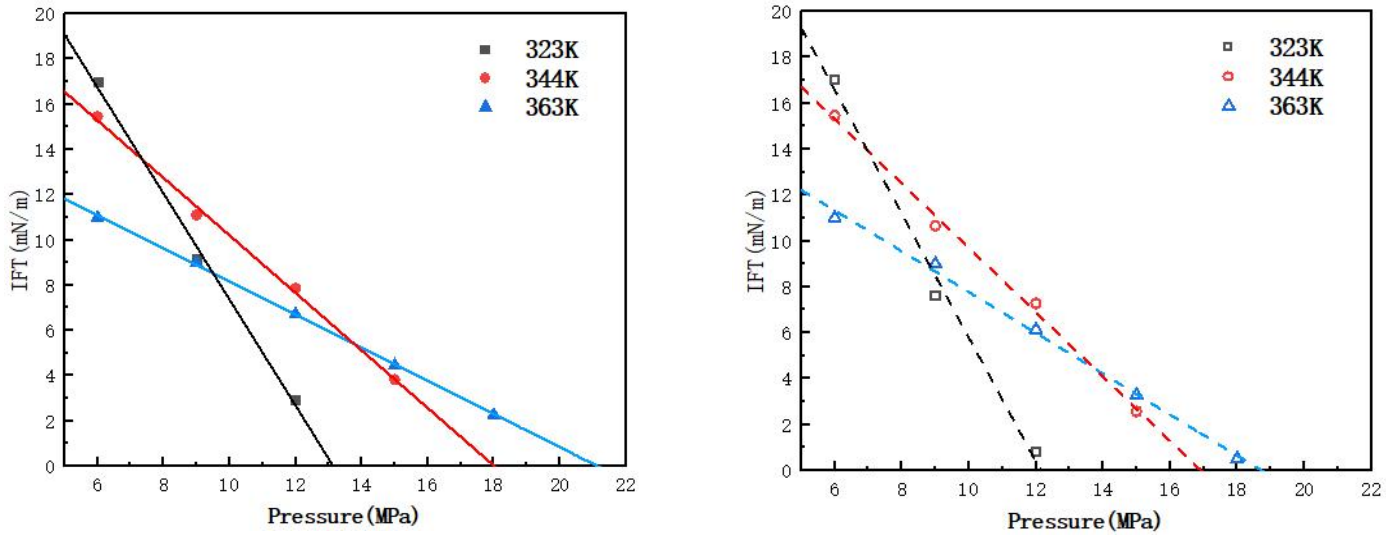

(a) CO_2+Oil system (b) CO_2+Oil+ $C_{12}PO_6$ system

Figure 10—Variations in interfacial tension within the oil displacement system at different temperatures.

In all three temperature conditions, an equal number of $C_{12}PO_6$ surfactant molecules were introduced (16 molecules in total, with eight molecules on each side of the crude oil phase). The minimum miscibility pressure (MMP) values before and after the addition of surfactants at each temperature were compared, and the results

are presented in **Table 2**. It is evident that an increase in temperature results in a greater reduction in the minimum miscibility pressure of the system. At 362K, the reduction is 10% higher compared to that at 323K.

Table 2—The minimum miscibility pressure for CO_2 flooding under different conditions.

Temperature, K	Minimum Miscibility Pressure, MPa		Reduction, %
	CO_2+oil	CO_2+oil +$C_{12}PO_6$	
323	12.81	12.13	5.29
344	18.65	16.90	9.38
363	21.32	18.06	15.29

Table 2 reveals that within the reservoir temperature range, the minimum miscibility pressure for CO_2 flooding increases as the temperature rises. However, the addition of surfactant demonstrates more effective performance. At a temperature of 363 K, the reduction in minimum miscibility pressure is notably higher compared to that at 323 K. Therefore, within this temperature range, reservoirs with higher temperatures are better suited for utilizing surfactants as additives to enhance oil recovery.

Conclusions

This study utilized molecular dynamics simulations to construct systems consisting of CO_2 and oil, as well as CO_2, oil, and a surfactant ($C_{12}PO_6$). Interface tensions were computed at different pressures under constant temperature for both systems. The minimum miscibility pressure was determined using the interface disappearance method, and the research focused on investigating how non-ionic surfactants reduce the minimum miscibility pressure. The investigation was primarily conducted by examining instantaneous phase-separation trajectories, density distributions, and radial distribution functions. These analyses shed light on the mechanisms at play in the interactions between CO_2 and crude oil, as well as the impact of surfactants in CO_2-oil systems. The key findings are as follows:

(1) The addition of surfactants noticeably widens the oil-phase interface and increases its volume occupancy. Surfactant molecules added to the system adsorb at the interface between crude oil and CO_2, forming a molecular film that enhances the interaction forces between the two, resulting in an expanded interface width.

(2) Surfactants can effectively reduce the minimum miscibility pressure (MMP) of the CO_2-crude oil system, facilitating the achievement of miscibility at lower reservoir pressures, thereby enhancing recovery (at a reservoir temperature of 344K, the reduction is increased by 9.36%).

(3) Temperature is a crucial factor affecting the effectiveness of recovery. With increasing reservoir temperature, the minimum miscibility pressure (MMP) for CO_2 and crude oil tends to rise, making it more difficult to achieve miscibility. However, at higher temperatures, the addition of surfactants leads to a more substantial reduction in MMP, enhancing their effectiveness in lowering MMP (at 363K, the decrease in temperature is enhanced by 10% compared to 323K).

Acknowledgments

This research was funded by the Open Foundation of the Shaanxi Key Laboratory of Carbon Dioxide Sequestration and Enhanced Oil Recovery. Additionally, the work was supported by the PetroChina Innovation Foundation (Grant number 2022DQ020201). The research also includes several specific projects: the study on

the mechanism of rod-tubing corrosion and wear in CO_2 solution based on machine learning (Project number YJSYZX23SKF0002), the study on the optimization of flowback models and regimes for shale gas post-fracturing (Project number GSYKY-B09-33), the evaluation of shale gas horizontal well productivity based on machine learning (Project number RIPED-2022-JS-1477), the evaluation methods and optimization of production regimes for two-phase flow in multi-stage fractured horizontal wells for shale gas (Project number RIPED-2023-JS-29), and the optimization of nozzle operating regimes for shale gas horizontal wells (Project number PGWX-202401).

Conflicting Interests

The author(s) declare that they have no conflicting interests.

References

Almobarak, M., Wu, Z., Zhou, D., et al. 2021. A Review of Chemical-Assisted Minimum Miscibility Pressure Reduction in CO_2 Injection for Enhanced Oil Recovery. *Petroleum* **7**(1):245-253.

Djabbarah, N.F. 1990. Miscible Oil Recovery Process Using Carbon Dioxide and Alcohol. US Patent US4899817A.

Dong, Z., Ma, X., Xu, H., et al. 2022. Molecular Dynamics Study of Interfacial Properties for Crude Oil with Pure and Impure CH_4. *Applied Sciences* **12**(1):12239.

Dong, Z., Qian, S., Li, W., et al. 2024. Molecular Dynamics Simulation of Surfactant Reducing MMP Between CH_4 and n-Decane. *Heliyon* **10**(1): 26441.

Fath, A.H. and Pouranfard, A.R. 2014. Evaluation of Miscible and Immiscible CO_2 Injection in One of the Iranian Oil Fields. Egyptian *Journal of Petroleum* **23**(1): 255-270.

Gozalpour, F., Ren, S. R., Tohidi, B. 2005. CO_2 EOR and Storage in Oil Reservoir. *Oil & Gas Science and Technology* **60**: 537-546.

Hoover, W.G., Ladd, A. J. C., Moran, B. 1982. High-Strain-Rate Plastic Flow Studied via Nonequilibrium Molecular Dynamics. *Physical Review Letters* **48**(1): 1818-1821.

Jorgensen, W.L., Maxwell, D.S., Tirado-Rives, J. 1996. Development and Testing of the OPLS All-Atom Force Field on Conformational Energetics and Properties of Organic Liquids. *Journal of the American Chemical Society* **118**(1): 11225-11236.

Ju, B., Wu, Y.S., Qin, J., et al. 2012. Modeling CO_2 Miscible Flooding for Enhanced Oil Recovery. *Petroleum Science* **9**(1): 192-198.

Lennard-Jones, J.E., 1931. Cohesion. *Proceedings of the Physical Society* **43**(1): 461-482.

Li, Q., Zhang, Z., Zhong, C., et al. 2003. Solubility of Solid Solutes in Supercritical Carbon Dioxide with and without Cosolvents. *Fluid Phase Equilibria* **207**(1): 183-192.

Li, W., Xu, H., Ma, X., et al. 2023. Molecular Dynamics-Based Analysis of the Factors Influencing the CO2 Replacement of Methane Hydrate. *Journal of Molecular Graphics and Modelling* **119**(1): 108394.

Lou, H., Zeng, M., Hu, Q., et al. 2018. Nonionic Surfactants Enhanced Enzymatic Hydrolysis of Cellulose by Reducing Cellulase Deactivation Caused by Shear Force and Air-Liquid Interface. *Bioresource Technology* **249**(1): 1-8.

Martin, M.G. and Siepmann, J. I. 1998. Transferable Potentials for Phase Equilibria. 1. United-Atom Description of n-Alkanes. *Journal of Physical Chemistry B* **102**(1): 2569-2577.

Miao, Y., Tang, L., and Gao, Z. 2013. Study on Affecting Factors of Water Cut Rising Rules of Horizontal Wells in Edge Water Reservoir. *Reservoir Evaluation and Development* **3**: 41-46.

Mo, Z., Li, Y., Fan, P. 2015. Effect of Online Reviews on Consumer Purchase Behavior. *Journal of Service Science and Management* **8**(1): 419-424.

Nath, S. K., Escobedo, F. A., and de Pablo, J. J. 1998. On the Simulation of Vapor–Liquid Equilibria for Alkanes. *Journal of Chemical Physics* **108**(1): 9905-9911.

Nosé, S. 1984. A Unified Formulation of the Constant Temperature Molecular Dynamics Methods. *Journal of Chemical Physics* **81**(1): 511-519.

Qi, G., Zhou, L., Long, M., et al. 2016. Experimental Study of the CO_2 Miscible Modulator Oil-Displacement Mechanism. *Science Technology and Engineering* **16**(35): 180-183.

Qu, B., Ma, X., Dong, Z. 2022. Interfacial Characterization and Minimum Miscible Pressure Study of CO_2 Flooding Based on Molecular Dynamics. *Improved Oil and Gas Recovery* **6**(1):1-15.

Rao, D.N. 1997. A New Technique of Vanishing Interfacial Tension for Miscibility Determination. *Fluid Phase Equilibria* **139**(1): 311-324.

Rudyk, S., Hussain, S., and Spirov, P. 2013. Supercritical Extraction of Crude Oil by Methanol- and Ethanol-Modified Carbon Dioxide. *Journal of Supercritical Fluids* **78**(1): 63-69.

Stanishneva-Konovalova, T.B. and Sokolova, O.S. 2015. Molecular Dynamics Simulations of Negatively Charged DPPC/DPPI Lipid Bilayers at Two Levels of Resolution. *Computational and Theoretical Chemistry* **1058**(1): 61-66.

Stukowski, A., Sadigh, B., Erhart, P., et al. 2009. Efficient Implementation of the Concentration-Dependent Embedded Atom Method for Molecular Dynamics and Monte Carlo Simulations. Modelling Simul. *Mater. Sci. Eng.* **17**(1): 075005.

Voon, C.L. and Awang, M.S.B. 2014. Reduction of MMP Using Oleophilic Chemicals. *World Academy of Science, Engineering and Technology, International Journal of Chemical, Molecular, Nuclear, Materials and Metallurgical Engineering* **8**(1): 351-353.

Wang, F., Luo, H., Ren, Y., et al. 2016. Influences of Fatty Alcohol Polyoxypropylene Ether on the Minimum Miscibility Pressure of Carbon Dioxide Flooding. *Petroleum Geology and Oilfield Development in Daqing* **35**(1): 118-122.

Wang, R., Peng, F., Song, K., et al. 2018. Molecular Dynamics Study of Interfacial Properties in CO_2 Enhanced Oil Recovery. *Fluid Phase Equilibria* **474**(1): 176-183.

Yang, S.Y., Lian, L.M., Yang, Y.Z., et al. 2015. Molecular Optimization Design and Evaluation of Miscible Processing Aids Applied to CO2 Flooding. *Xinjiang Petroleum Geology* **36**(5): 555-559.

Yang, Z., Wu, W., Dong, Z., et al. 2019. Reducing the Minimum Miscibility Pressure of CO_2 and Crude Oil Using Alcohols. *Colloids and Surfaces A: Physicochemical and Engineering Aspects* **568**(1):105-112.

Zhu, A., Zhang, X., Liu, Q., et al. 2009. A Fully Flexible Potential Model for Carbon Dioxide. *Chinese Journal of Chemical Engineering* **17**(1): 268-272.

Zhenzhen Dong, is a Professor in the Petroleum Engineering Department at Xi'an Shiyou University. Her research interests include unconventional resources/reserves estimates, reservoir simulation, well testing, and production analysis. Dr. Dong holds a bachelor's degree in mathematics from Northeast Petroleum University, China; a master's degree in petroleum engineering from Research Institute of Petroleum Exploration and Development, China; and a PhD degree in petroleum engineering from Texas A&M University.

Tong Hou, is a master candidate in Petroleum Engineering department at Xi'an Shiyou University. She has focuses her research in areas involving molecular dynamic simulation and enhanced oil recovery.

Zhanrong Yang, is a master candidate in Petroleum Engineering department at Xi'an Shiyou University. His research focuses on reservoir simulation and enhanced oil recovery.

Lu Zou, is a master candidate in Petroleum Engineering department at Xi'an Shiyou University. His research involves machine learning, reservoir simulation,and enhanced oil recovery.

Weirong Li, is a Professor in the Petroleum Engineering Department at Xi'an Shiyou University. His research interests include unconventional resources/reserves estimates, reservoir simulation, well testing, and production analysis. Dr. Li holds a bachelor's degree in Petroleum Engineering from Northeast Petroleum University, China; a master's degree in petroleum engineering from Research Institute of Petroleum Exploration and Development, China; and a PhD degree in petroleum engineering from Texas A&M University.

Keze Lin, is a undergraduate student of China University of Petroleum (Beijing), Beijing. He focuses on enhanced oil recovery and reservoir engineering.

Hongliang Yi, is a senior reservoir engineer in Liaohe Oilfield Company of PetroChina. He specializes in enhanced oil recovery and production analysis.

Zhilong Liu is a senior reservoir engineer in EnerTech-Drilling & Production Co., CNOOC Energy Technology & Services Ltd. His specialties include reservoir management and enhance oil recovery.